Centralized Cooperative Positioning and Tracking with Realistic Communications Constraints

Mensing, Christian; Nielsen, Jimmy Jessen

Published in:
7th Workshop on Positioning Navigation and Communication (WPNC), 2010

DOI (link to publication from Publisher):
10.1109/WPNC.2010.5651897

Publication date:
2010

Document Version
Accepted author manuscript, peer reviewed version

Centralized Cooperative Positioning and Tracking with Realistic Communications Constraints

Christian Mensing
German Aerospace Center (DLR)
Institute of Communications and Navigation
Oberpfaffenhofen, 82234 Wessling, Germany
E-mail: christian.mensing@dlr.de

Jimmy Jessen Nielsen
Aalborg University
Department of Electronic Systems, Networking and Security
Fredrik Bajers vej 7, 9220 Aalborg, Denmark
E-mail: jjn@es.aau.dk

***Abstract*—In this paper, we investigate the performance of centralized cooperative positioning algorithms. Compared to traditional positioning algorithms which solely exploit ranging information from anchor nodes, cooperative positioning additionally uses measurements from peer-to-peer links between the users. Since we are proposing a centralized architecture, all information has to be collected at a central entity for position calculation and further provision to the network. Hence, besides position-relevant metrics like accuracy and coverage also communications overhead and latency and their impact on the overall performance will be assessed. As we are considering a dynamic scenario, the cooperative positioning algorithms are based on extended Kalman filtering for position estimation and tracking. Simulation results for ultra-wideband based ranging information and WLAN based communications infrastructure show the benefits of cooperative position and tracking for realistic measurement and mobility models.**

I. Introduction

Services and applications based on accurate location knowledge of mobile stations (MSs) will play fundamental roles in future wireless systems. Hence, provision and exploitation of MS position information have become very important features of communications systems in recent years [1]. To meet the accuracy and coverage requirements for reliable position estimation, global navigation satellite systems (GNSSs) — like the Global Positioning System (GPS) and the future European Galileo system — can deliver very good position estimates under optimum conditions [2]. However, especially in critical positioning scenarios like urban canyons or indoor environments the performance loss can be very high [3] or GNSS based positioning is even not possible.

As solution for 'GNSS-supporting' or even 'GNSS-free' position estimation, already available communications systems can be part of the MS localization process [1]. In these systems, measurements in terms of time of arrival (TOA), time difference of arrival (TDOA), angle of arrival (AOA), or received signal strength (RSS), provided by the anchor nodes (ANs) or the MS can be used. A following hybrid and/or heterogeneous data fusion (HDF) of these measurements will give reliable position estimates of the MSs in the network.

For two-dimensional positioning it is required that the MS can perform measurements with at least three ANs. If links are blocked (e.g., by walls in dense indoor environments) or the geometric conditions are restricted the MS might not be able to determine its position accurately. For such situations a cooperative approach can be recommended, where MSs can communicate via peer-to-peer (P2P) links with each other. On the one hand, that allows the direct exchange of position information between neighboring MSs. On the other hand, these P2P links can be used to derive distance information between these MSs which can be further exploited for position estimation. This cooperative positioning (CP) approach helps to improve the performance in terms of accuracy and coverage compared to conventional HDF techniques.

The concept of CP, mostly applied nowadays to wireless sensor networks (WSNs), has been recently introduced to heterogeneous communications systems. However, techniques proposed for WSN cannot be straightforwardly extended to mobile communications networks. This is because these networks usually operate in a very complex and harsh wireless environment due to factors such as shadowing, mobility, communications infrastructure, or multiple air-interfaces. Hence, the heterogeneity of today's wireless communication networks can be seen as an additional problem to be addressed.

In principle, there are two different procedures: in the centralized approach of CP (e.g., [4], [5]) it is assumed that all information (i.e., the measurements collected by the MSs) is provided to one central entity. That could be a location server in a cellular communications system. There, the measurements are jointly processed and the position for each MS in the network is determined. Afterwards, this information can be exploited in the network or sent back to the MSs. As all measurements are processed jointly in this approach, it is the optimum procedure from a position estimation accuracy point of view. However, drawback is that all measurements have to be collected at a central entity in advance. So as to cope with scalability in dense large-scale networks or for MS-centric applications using restricted infrastructure, the distributed CP approach can also be favored as an alternative to centralized methods (e.g., [6], [7]). Here, the MSs have only the information available that they obtain from their neighbors via P2P links and the measurements with the ANs. Hence, the position estimation complexity is distributed among the MSs compared to the centralized approach. An extensive overview of CP techniques discussed under the framework of Bayesian inference can be found in [6].

Generally, the communications overhead and extra-signalling is higher for cooperative approaches than for conventional (non-cooperative) positioning. Furthermore, usually the overall overhead of distributed schemes is higher than for centralized schemes. Hence, signal-processing complexity and training/signalling overhead are two key problems for existing CP approaches. This problem can be significant especially for a wireless network accommodating a large number of MSs. Therefore, an efficient CP scheme should achieve the best trade-off between communications overhead and position estimation performance.

In this paper, we investigate the performance of a centralized CP scheme under realistic communications constraints and measurement models from both the positioning and the communications perspective. The centralized infrastructure is based on WLAN collecting the measurements between the ANs and the MSs as well as the P2P measurements between the MSs. The ranging is realized by ultra-wideband (UWB) TOA measurements. Additionally, mobility of the users is exploited by application of tracking algorithms based on extended Kalman filters (EKFs). Hence, simulation results will provide a realistic assessment of centralized CP in a high-mobility environment.

Section II introduces the system model of cooperative positioning exploiting measurements from ANs and P2P links. In Section III static and dynamic CP algorithms are described for a centralized infrastructure. Section IV describes the proposed communications infrastructure for exchanging MS-MS and MS-AN measurements including the underlying protocols as well as the assumed models in this paper. In Section V the simulation approach for combining the communications part with the positioning part is presented. Finally, Section VI discusses the simulation results.

Throughout this paper, vectors and matrices are denoted by lower and upper case bold letters, the operation '$\otimes$' denotes the Kronecker product, $(\cdot)^{\mathrm{T}}$ the transpose operation, and $\mathrm{E}\{\cdot\}$ expectation. The Euclidean norm is denoted as $\|\cdot\|_2$, and the N-dimensional identity matrix is denoted as $\mathbf{I}_N$.

II. System model

We consider N_{AN} ANs and N_{MS} MSs that are present in the scenario. The ANs are located at the known and fixed positions

$$\boldsymbol{x}^{(\mathrm{AN})} = \begin{bmatrix} \boldsymbol{x}_1^{(\mathrm{AN}),\mathrm{T}} & \boldsymbol{x}_2^{(\mathrm{AN}),\mathrm{T}} & \dots & \boldsymbol{x}_{N_{\mathrm{AN}}}^{(\mathrm{AN}),\mathrm{T}} \end{bmatrix}^{\mathrm{T}}, \quad (1)$$

where

$$\boldsymbol{x}_\mu^{(\mathrm{AN})} = \begin{bmatrix} x_\mu^{(\mathrm{AN})} & y_\mu^{(\mathrm{AN})} \end{bmatrix}^{\mathrm{T}}, \quad \mu = 1, 2, \dots, N_{\mathrm{AN}}, \quad (2)$$

describes the position of the AN μ. The positions of the MSs

$$\boldsymbol{x} = \begin{bmatrix} \boldsymbol{x}_1^{\mathrm{T}} & \boldsymbol{x}_2^{\mathrm{T}} & \dots & \boldsymbol{x}_{N_{\mathrm{MS}}}^{\mathrm{T}} \end{bmatrix}^{\mathrm{T}} \quad (3)$$

with

$$\boldsymbol{x}_\nu = \begin{bmatrix} x_\nu & y_\nu \end{bmatrix}^{\mathrm{T}}, \quad \nu = 1, 2, \dots, N_{\mathrm{MS}}, \quad (4)$$

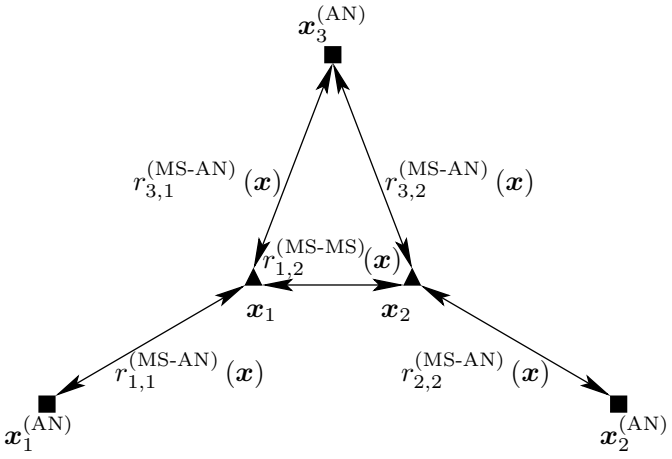

Fig. 1. Cooperative positioning principle

have to be estimated. Note that we restrict to a two-dimensional scenario in this paper, however, an extension to three-dimensional approaches is straightforward.

The range between the MS ν and the AN μ can be calculated as

$$r_{\nu,\mu}^{(\mathrm{MS\text{-}AN})}(\boldsymbol{x}) = \sqrt{\left(x_\mu^{(\mathrm{AN})} - x_\nu\right)^2 + \left(y_\mu^{(\mathrm{AN})} - y_\nu\right)^2} \quad (5)$$

and the range between the MSs ν and $\nu' \neq \nu$ is given as

$$r_{\nu,\nu'}^{(\mathrm{MS\text{-}MS})}(\boldsymbol{x}) = \sqrt{(x_\nu - x_{\nu'})^2 + (y_\nu - y_{\nu'})^2}, \quad (6)$$

where the dependence on the MS positions is explicitly denoted by $\boldsymbol{x}$. An overview of the CP principle with three ANs and two MSs is depicted in Figure 1.

The ranging error model for the MS-AN measurements can be written as

$$\hat{r}_{\nu,\mu}^{(\mathrm{MS\text{-}AN})} = r_{\nu,\mu}^{(\mathrm{MS\text{-}AN})}(\boldsymbol{x}) + b_{\nu,\mu}^{(\mathrm{MS\text{-}AN})} + n_{\nu,\mu}^{(\mathrm{MS\text{-}AN})}, \quad (7)$$

where the bias $b_{\nu,\mu}^{(\mathrm{MS\text{-}AN})}$ and the residual noise $n_{\mu,\nu}^{(\mathrm{MS\text{-}AN})}$ depend on the LOS/NLOS status and the distance. Whereas the MS index $\nu = 1, \dots, N_{\mathrm{MS}}$ includes all MSs in the network, the AN index for each MS $\mu = 1, \dots, N_{\mathrm{AN,\,Used},\nu}$ includes only the $N_{\mathrm{AN,\,Used},\nu} < N_{\mathrm{AN}}$ ANs which can be used for ranging from MS ν. Equivalently, the ranging error model for the MS-MS measurements is given as

$$\hat{r}_{\nu,\nu'}^{(\mathrm{MS\text{-}MS})} = r_{\nu,\nu'}^{(\mathrm{MS\text{-}MS})}(\boldsymbol{x}) + b_{\nu,\nu'}^{(\mathrm{MS\text{-}MS})} + n_{\nu,\nu'}^{(\mathrm{MS\text{-}MS})}, \quad (8)$$

where $\nu' = 1, \dots, N_{\mathrm{MS,\,Used},\nu}$ includes the available other MSs of MS ν for performing ranging.

We include all available MS-AN and MS-MS measurements in the vector

$$\hat{\boldsymbol{r}} = \begin{bmatrix} \hat{\boldsymbol{r}}^{(\mathrm{MS\text{-}AN}),\mathrm{T}} & \hat{\boldsymbol{r}}^{(\mathrm{MS\text{-}MS}),\mathrm{T}} \end{bmatrix}^{\mathrm{T}} \quad (9)$$

of dimension

$$N_{\mathrm{Used}} = N_{\mathrm{AN,\,Used}} + N_{\mathrm{MS,\,Used}} \quad (10)$$

with

$$N_{\text{AN, Used}} = \sum_{\nu=1}^{N_{\text{MS}}} N_{\text{AN, Used},\nu} \tag{11}$$

and

$$N_{\text{MS, Used}} = \sum_{\nu=1}^{N_{\text{MS}}} N_{\text{MS, Used},\nu}. \tag{12}$$

With the equivalent definitions of the range vector $\boldsymbol{r}(\boldsymbol{x})$, the bias vector $\boldsymbol{b}$, and the noise vector $\boldsymbol{n}$ with covariance matrix

$$\boldsymbol{\Sigma}_n = \begin{bmatrix} \boldsymbol{\Sigma}_n^{(\text{MS-AN})} & \mathbf{0} \\ \mathbf{0} & \boldsymbol{\Sigma}_n^{(\text{MS-MS})} \end{bmatrix}, \tag{13}$$

we arrive at the compact measurement model

$$\hat{\boldsymbol{r}} = \boldsymbol{r}(\boldsymbol{x}) + \boldsymbol{b} + \boldsymbol{n}. \tag{14}$$

III. Centralized cooperative positioning algorithms

A. Static solution

For the static solution of the centralized CP estimation problem, we follow the weighted non-linear least squares approach [8], [9] according to

$$\hat{\boldsymbol{x}} = \underset{\boldsymbol{x}}{\operatorname{argmin}} \left(\hat{\boldsymbol{r}} - \boldsymbol{r}(\boldsymbol{x})\right)^{\mathrm{T}} \boldsymbol{\Sigma}_n^{-1} \left(\hat{\boldsymbol{r}} - \boldsymbol{r}(\boldsymbol{x})\right). \tag{15}$$

In the general case, there exists no closed-form solution to this non-linear $2N_{\text{MS}}$-dimensional optimization problem, and hence, iterative approaches are necessary. A standard approach to deal with (15) is based on the Gauss-Newton (GN) algorithm [8], [9]. The GN algorithm linearizes the system model about some initial value $\boldsymbol{x}^{(0)}$ yielding

$$\boldsymbol{r}(\boldsymbol{x}) \approx \boldsymbol{r}\left(\boldsymbol{x}^{(0)}\right) + \boldsymbol{\Phi}(\boldsymbol{x})\Big|_{\boldsymbol{x}=\boldsymbol{x}^{(0)}} \left(\boldsymbol{x} - \boldsymbol{x}^{(0)}\right), \tag{16}$$

with the elements of the $N_{\text{Used}} \times 2N_{\text{MS}}$ Jacobian matrix

$$\boldsymbol{\Phi}(\boldsymbol{x}) = \nabla_{\boldsymbol{x}}^{\mathrm{T}} \otimes \boldsymbol{r}(\boldsymbol{x}), \tag{17}$$

where

$$\nabla_{\boldsymbol{x}} = \left[\frac{\partial}{\partial x_1}, \frac{\partial}{\partial y_1}, \ldots, \frac{\partial}{\partial x_{N_{\text{MS}}}}, \frac{\partial}{\partial y_{N_{\text{MS}}}}\right]^{\mathrm{T}}. \tag{18}$$

Afterwards, the linear least squares procedure is applied resulting in the iterated solution

$$\begin{aligned} \boldsymbol{x}^{(k+1)} = \boldsymbol{x}^{(k)} + &\left(\boldsymbol{\Phi}^{\mathrm{T}}\left(\boldsymbol{x}^{(k)}\right) \boldsymbol{\Sigma}_n^{-1} \boldsymbol{\Phi}\left(\boldsymbol{x}^{(k)}\right)\right)^{-1} \\ &\cdot \boldsymbol{\Phi}^{\mathrm{T}}\left(\boldsymbol{x}^{(k)}\right) \boldsymbol{\Sigma}_n^{-1} \left(\hat{\boldsymbol{r}} - \boldsymbol{r}\left(\boldsymbol{x}^{(k)}\right)\right). \end{aligned} \tag{19}$$

The GN algorithm provides very fast convergence and accurate estimates for good initial values. For poor initial values and bad geometric conditions the algorithm results in a rank-deficient, and thus, non-invertible matrix for certain geometric constellations of MSs and ANs.

For the considered approach, the initial value for the individual MSs is defined by the mean value of the positions of the visible ANs, i.e., corresponding to

$$\boldsymbol{x}_\nu^{(0)} = \frac{1}{N_{\text{AN, Used},\nu}} \sum_{\mu=1}^{N_{\text{AN, Used},\nu}} \boldsymbol{x}_\mu^{(\text{AN})}. \tag{20}$$

B. Extended Kalman filter

Usually the MSs are moving along certain tracks in the scenario. Clearly, there are strong correlations between the positions of the MSs over time. This information will be integrated in the overall position determination process and will help to improve the overall estimates in average. The Kalman filter (KF) [8] is a flexible and well-known algorithm for providing such positioning estimates in the context of MS tracking applications. However, the standard KF only performs optimum if the criterions on linearity and Gaussianity are fulfilled, which is usually not the case in practical MS tracking applications. Even if these conditions are not fulfilled completely, the KF gives reliable and robust estimates.

The main drawback of the linear KF is that it requires a linear state-space equation and a linear observation model (in addition to zero-mean Gaussian noise processes) to perform optimum. Clearly, for tracking only the position of the MS based on recent position estimates and the mobility model would result in such a linear relation. However, if we want to include direct range measurements that have a high non-linear property w.r.t. the current positions, the linear KF is not a reasonable approach to solve this problem.

Therefore, we propose an EKF implementation [8], [10]. The inherent combination of CP and tracking has the further advantage that also recent estimates are considered in the position estimation process corresponding to the chosen mobility model. The EKF is based on a linearized KF and gives a good trade-off between accuracy, robustness, and complexity [8]. The state-space and observation models are

$$\begin{aligned} \boldsymbol{s}[k] &= \boldsymbol{A}\boldsymbol{s}[k-1] + \boldsymbol{u}[k] \\ \hat{\boldsymbol{r}}[k] &= \boldsymbol{h}(\boldsymbol{s}[k]) + \boldsymbol{n}[k], \end{aligned} \tag{21}$$

where

$$\boldsymbol{s}[k] = \begin{bmatrix} \boldsymbol{x}_1^{\mathrm{T}} & \boldsymbol{v}_1^{\mathrm{T}} & \boldsymbol{x}_2^{\mathrm{T}} & \boldsymbol{v}_2^{\mathrm{T}} & \ldots & \boldsymbol{x}_{N_{\text{MS}}}^{\mathrm{T}} & \boldsymbol{v}_{N_{\text{MS}}}^{\mathrm{T}} \end{bmatrix}^{\mathrm{T}} \tag{22}$$

is the $4N_{\text{MS}}$-dimensional state-space vector in each time-step $k \in \mathbb{N}$, including two-dimensional positions and velocities of each MS as parameters that have to be estimated. The vector $\hat{\boldsymbol{r}}[k]$ includes the ranging measurements for each time-step and changes over time depending on the availability of the measurements. The matrix

$$\boldsymbol{A} = \left(\mathbf{I}_4 + \left(\begin{bmatrix} T & 0 \\ 0 & T \end{bmatrix} \otimes \begin{bmatrix} 0 & 1 \\ 0 & 0 \end{bmatrix}\right)\right) \otimes \mathbf{I}_{N_{\text{MS}}} \tag{23}$$

includes apriori information about the MS movements with timing updates every T time-steps. The vector $\boldsymbol{u}[k]$ is composed of state-space noise with the diagonal covariance matrix $\boldsymbol{Q}$, and $\boldsymbol{n}[k]$ is composed of the observation noise with the covariance matrix $\boldsymbol{\Sigma}_n[k]$. The covariance matrix can change dynamically over time depending on number and type of available measurements. Finally, the function $\boldsymbol{h}(\cdot)$ describes the non-linear relation between the state-space vector and the measurements.

The equations for the state-space and observation models in (21) are then used to set-up the EKF. It starts with the

prediction, where knowledge of the MS movement model is applied to obtain

$$\hat{\boldsymbol{s}}\left[k|k-1\right] = \boldsymbol{A}\hat{\boldsymbol{s}}\left[k-1|k-1\right], \tag{24}$$

with the estimate of the previous time-step $\hat{\boldsymbol{s}}\left[k-1|k-1\right]$. Similarly, the corresponding minimum mean square error (MMSE) matrix after that prediction step is

$$\boldsymbol{M}\left[k|k-1\right] = \boldsymbol{A}\boldsymbol{M}\left[k-1|k-1\right]\boldsymbol{A}^{\mathrm{T}} + \boldsymbol{Q}. \tag{25}$$

Note that the EKF iterations are initialized by a static solution at the beginning. Further, we observe that in the chosen implementation the mobility of the different MSs is decoupled, i.e., for the filter equations it is assumed that the MSs move independently of each other. The Kalman gain matrix includes a weighting between the predicted estimates and the current measurements. It is given as

$$\begin{aligned}\boldsymbol{K}\left[k\right] &= \boldsymbol{M}\left[k|k-1\right]\boldsymbol{H}^{\mathrm{T}}\left[k\right] \\ &\cdot \left(\boldsymbol{\Sigma}_n\left[k\right] + \boldsymbol{H}\left[k\right]\boldsymbol{M}\left[k|k-1\right]\boldsymbol{H}^{\mathrm{T}}\left[k\right]\right)^{-1},\end{aligned} \tag{26}$$

where — equivalent to $\boldsymbol{\Sigma}_n\left[k\right]$ — the dimensions can change over time. In the classical KF equations the matrix $\boldsymbol{H}\left[k\right]$ includes a linear relation between state-space and measurement model. Since for positioning applications we usually have a non-linear dependency, the observation equation is linearized around the predicted state-space vector, i.e.,

$$\boldsymbol{h}\left(\boldsymbol{s}\left[k\right]\right) \approx \boldsymbol{h}\left(\hat{\boldsymbol{s}}\left[k|k-1\right]\right) + \boldsymbol{H}\left[k\right]\left(\boldsymbol{s}\left[k\right] - \hat{\boldsymbol{s}}\left[k|k-1\right]\right), \tag{27}$$

where the Jacobian observation matrix is

$$\boldsymbol{H}\left[k\right] = \left.\frac{\partial \boldsymbol{h}\left(\boldsymbol{s}\left[k\right]\right)}{\partial \boldsymbol{s}\left[k\right]}\right|_{\boldsymbol{s}[k]=\hat{\boldsymbol{s}}[k|k-1]}, \tag{28}$$

which easily can be derived from $\boldsymbol{\Phi}\left(\boldsymbol{x}\right)$. Hence, it includes the derivations of the observation equation w.r.t. the variables of the state-space vector. Finally, the correction step combines the predicted estimates with the current measurements weighted with the Kalman gain matrix. This results in the final estimate of the state-space vector

$$\hat{\boldsymbol{s}}\left[k|k\right] = \hat{\boldsymbol{s}}\left[k|k-1\right] + \boldsymbol{K}\left[k\right]\left(\hat{\boldsymbol{r}}\left[k\right] - \boldsymbol{h}\left(\hat{\boldsymbol{s}}\left[k|k-1\right]\right)\right). \tag{29}$$

The corresponding MMSE matrix is obtained as

$$\boldsymbol{M}\left[k|k\right] = \left(\mathbf{I}_{4N_{\mathrm{MS}}} - \boldsymbol{K}\left[k\right]\boldsymbol{H}\left[k\right]\right)\boldsymbol{M}\left[k|k-1\right]. \tag{30}$$

The EKF is designed in a flexible way, i.e., different numbers of measurements can be exploited. They also can change online for the different time-steps. Even the situation that no AN or other MS is visible for a certain time can be handled by this approach. In that situation, the movement model compensates the missing measurements.

IV. Realistic Communication Constraints

We evaluate the conventional and cooperative localization algorithms described above under realistic communication constraints by considering: 1) the timing of measurement exchanges and availability of measurements through accurate simulations, as well as 2) realistic error model of UWB based P2P ranging, and finally 3) a group mobility model that mimics correlated user movements.

For both the conventional and the cooperative approaches for localization that are considered in this work we have defined protocols that are responsible for collection of measurements and provision of a location estimate. In the following we describe these protocols. In addition to collecting the measurements in the localization server, we assume that the location estimate is needed by an application at the MS, which polls the location every μ_{loc} seconds.

A. Measurement collection for device-based conventional localization

In this case, the localization algorithm uses only measurements from the MS-AN links as sketched in Fig. 2 which shows an example scenario with 4 ANs. As the MS holds all measurements necessary to compute the location estimate, we assume the localization/tracking algorithm is run in the MS.

Link measurements are obtained from IEEE 802.11 MAC beacons that are being broadcast in an unsynchronized manner from the ANs every μ_{beacon} seconds. Further, we assume that the transmit power P_{tx} is fixed, known and equal for all ANs. Depending on the transmit power level and the density of ANs used in a given scenario, the number of ANs within communication range of the MS and hence the number of received beacons will vary.

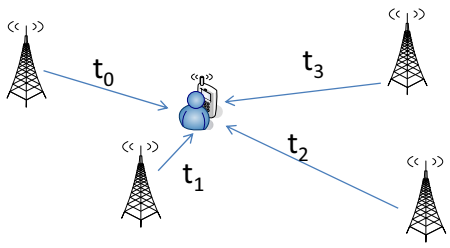

Fig. 2. Message flow in device-based conventional positioning.

Since the link measurements are obtained directly in the MS from the beacons transmitted from the ANs, the only factor that attributes to the localization delay is the application location request interval μ_{loc}.

B. Measurement collection for centralized cooperative localization

In addition to MS-AN link measurements, the cooperative localization algorithms uses MS-MS ranging measurements and centralized computation of location estimates. In order to realize the collection of both types of measurements, as well as send back the location estimate to the MS, the message flow sketched in Fig. 3 is used.

In order to show the message flow more clearly, we consider the subflows individually in the following.

Like the conventional algorithms, the cooperative algorithms rely on periodically transmitted beacons (every μ_{beacon} seconds) for MS-AN measurements. As before, we assume that the transmit power P_{tx} is fixed, known and equal for all

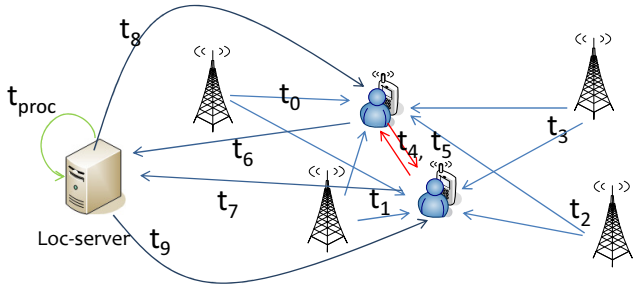

Fig. 3. Message flow in centralized cooperative positioning.

ANs. Fig. 4 shows how beacons transmitted from the ANs are first received and used for ranging at the MS. Hereafter a measurement packet, which contains the ranging measurement, is sent to the nearest AN and thereafter to the localization server, which is assumed to be connected to the AN by a wired infrastructure.

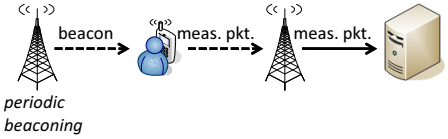

Fig. 4. Message flow for beacon measurements in cooperative localization.

In addition to MS-AN measurements, the cooperative algorithms rely on MS-MS measurements. The flow of messages is shown in Fig. 5. Whenever an MS senses another MS within d_{coop} meters, a P2P ranging measurement is made and sent to the localization server through the nearest AN. However, to reduce the amount of measurement packets being sent, P2P measurements are buffered and sent in a bundle every μ_{coop} seconds. As with the MS-AN measurements, the AN is assumed to be connected to the localization server by a wired infrastructure.

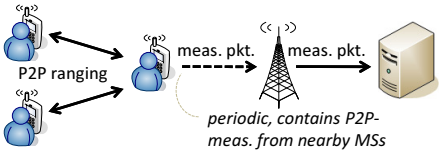

Fig. 5. Message flow for P2P measurements in cooperative localization.

Having both MS-AN and MS-MS measurements at the localization server, we now need to provide the calculated position estimate to the MS. This is done by unicasting a message with the current location estimate of an MS to that MS, whenever a beacon from the nearest AN is received, as sketched in Fig. 6.

The results in section VI shows the delays and transferred bytes for each of the message collection protocols.

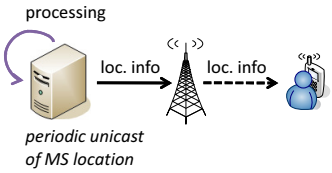

Fig. 6. Message flow for location info message in cooperative localization.

C. 802.11a WiFi network model

The 802.11a WiFi network is simulated using ns-2[1] based on the mobility trace and the scenario specific parameters listed in Table II. We use the *802.11ext* module to simulate realistic 802.11a behavior. This ns-2 version includes a Nakagami fading model which has been parameterized according to Table II with model parameters $\Gamma = n$ and $m = \frac{(K+1)^2}{2K+1}$, where K is the Ricean K-factor, to approximate a Ricean fading environment.

Table I shows the sizes of the used messages. We have made the following assumptions regarding the used messages. The beacon is a standard 802.11 MAC frame, which follows the frame layout defined in [12]. The beacon measurement is a 802.11 data frame with a payload consisting of the MAC id (6 bytes) of the AP and the estimated range (2 bytes). The P2P measurement bulk message size depends on the number of P2P neighbors in range. It is based on a data frame (28 bytes) where the payload is a 6 bytes MAC id and 2 bytes ranging value for each neighbor node. Finally, the location information message is a data frame with the node coordinates (x,y) encoded with 8 bytes each.

Message type	MPDU size (bytes)
802.11 MAC beacon	52
Beacon measurement	42
P2P measurement bulk	$28 + (6 + 2) \cdot N_{\text{MS in range}}$
Location information	44

TABLE I
MESSAGE TYPES

D. Measurement model

For modeling the ranging errors, we make use of a preliminary version of the models presented in [13]. It models bias and residual noise conditioned on distance, orientation, and LOS/NLOS status of the connection. The average standard deviation of noise and the average bias are depicted in Figure 7 over the distance for LOS and NLOS conditions.

E. Group mobility model

A variation of the random waypoint that mimics group mobility is used in this work. In each group of nodes, one of the nodes acts as the reference node. For this node a waypoint and speed is chosen as usual for the random waypoint model (see [14]). For the remaining nodes in the group the same

[1]The ns-2 simulation is based on [11], which has been updated with the author's patch from June 5th, 2009.

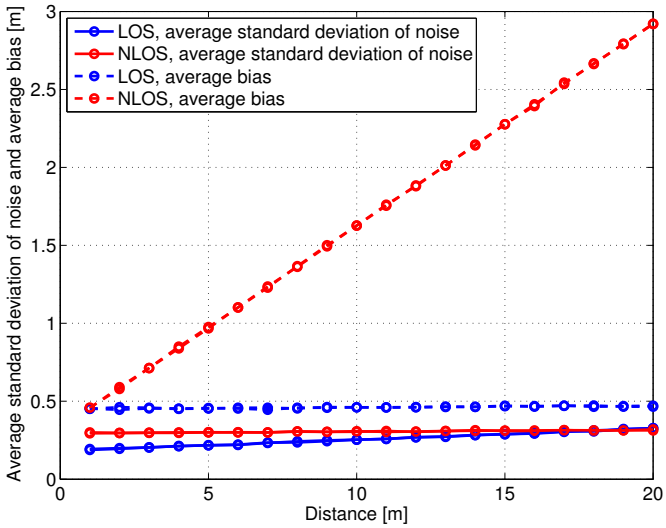

Fig. 7. Average ranging error model parameters vs. distance

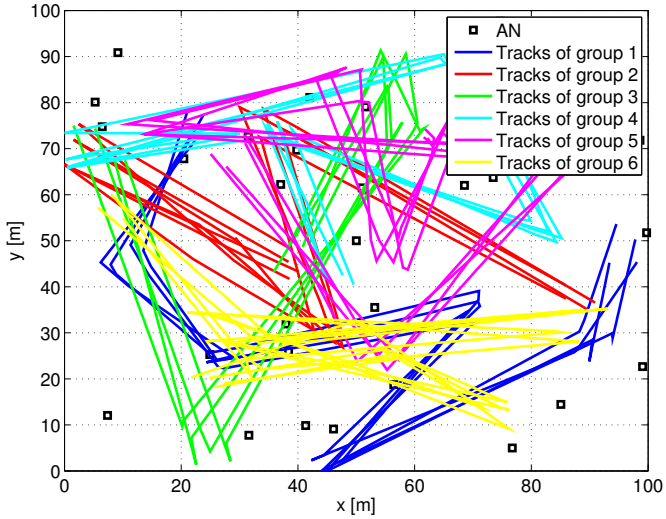

Fig. 8. Group mobility simulation example.

speed is used and a their waypoints are chosen, so that they are randomly placed within d_{spread} of the reference node's waypoint. An example of the resulting mobility tracks is shown in 8 in a $100x100m^2$ scenario. In this example there are 6 groups with 4 nodes in each group, shown with a unique color for each group.

V. Evaluation Methodology

The considered localization algorithms have been evaluated with realistic communications constraints in a 4-step process as sketched in Fig. 9. Initially, a common *Mobility simulation* is run, which results in a trace file that describes the AN positions and MS movements according to the random waypoint group mobility model described in section IV-E. This mobility trace is then used as a basis for simulating the message collection protocols in the ns-2 based *Network simulation*. The output of this step is first the network-related performance metrics, and secondly this block also delivers a trace file specifying time stamps for when measurements are obtained and have been collected, according to the collection protocol. Using this trace file in combination with the mobility trace, the actual measurement values for the MS-AN and MS-MS links are being generated in the *Measurement generation* block using the models described in section IV-D. Finally, the *Positioning simulation* is run and positioning metrics are computed for the considered conventional and cooperative localization algorithms.

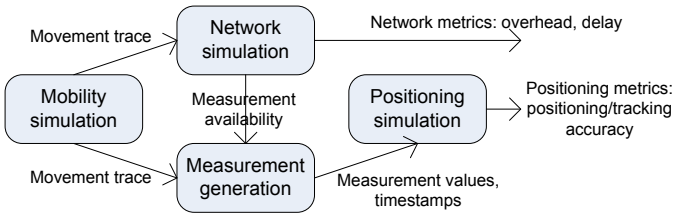

Fig. 9. Simulation overview.

VI. Simulation Results

The baseline simulation parameters are concluded in Table II.

Parameter	Value
Time	100 s
Size	$100x100m^2$
Number of ANs (N_{AN})	30
Number of MS groups (N_{groups})	6
Number of MSs per group ($N_{\text{MS/group}}$)	4
Max spread relative to ref. MS in group (d_{spread})	20 m
Movement speed ($\|\mathbf{v}\|$)	2 m/s
AN beacon interval (μ_{beacon})	1 s
P2P ranging interval (μ_{coop})	1 s
P2P ranging distance (d_{coop})	20 m
Location information update interval ($\mu_{\text{loc-info}}$)	1 s
MS application request interval (μ_{loc})	1 s
Localization processing time (μ_{proc})	0.1 s
Path loss exponent (n)	2.9
Rician K-factor (K)	6
Transmit power (P_{tx})	5 mW
802.11a PHY mode	6 Mbit/s, BPSK
Bandwidth	20 MHz
Frequency	5.18 GHz
Carrier Sense Threshold	-92 dBm
Noise floor	-106 dBm

TABLE II
Network Simulation Parameters

We start with the evaluation of communications metrics. Next we consider the positioning algorithms; first assuming perfect communications, i.e., error-free and instantaneous exchange of all required information, and secondly we introduce the realistic communications constraint.

A. Communications part

Initially we consider the effect of varying the transmit power. Fig. 10 confirms that the number of ANs within

carrier sense for each MS range increases with the transmit power, as expected. Notice that the curves for conventional and cooperative are (unsurprisingly) identical.

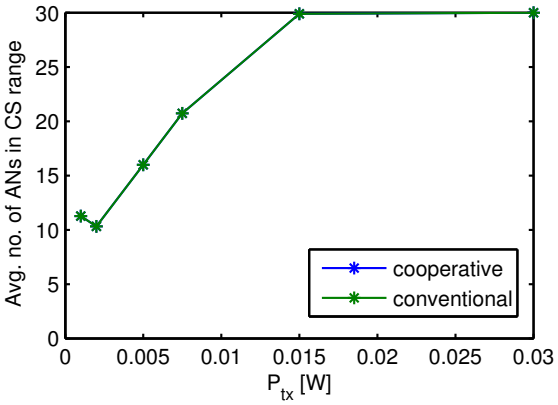

Fig. 10. The number of ANs within carrier sense range for varying transmit power level.

In Fig. 11 we show the average fraction of occupied channel time per AN. This metric is calculated by summing the time spent on transmissions within carrier sense range of each AN. The AN may overhear multiple simultaneous transmissions, since the considered $100x100m^2$ scenario does not constitute a single collision domain. In this plot it is clearly shown that the amount of occupied channel around each AN for the conventional measurement collection is much less than for the cooperative. Since the number of ANs and MSs is similar for conventional and cooperative, we can conclude that the conventional algorithm uses much less capacity for signaling, as we would expect. Further, all entities seem to be within the same collision domain for both $P_{\text{tx}} = 0.015$ and $P_{\text{tx}} = 0.030$ since the fraction of occupied channel does not change between these two parameter settings.

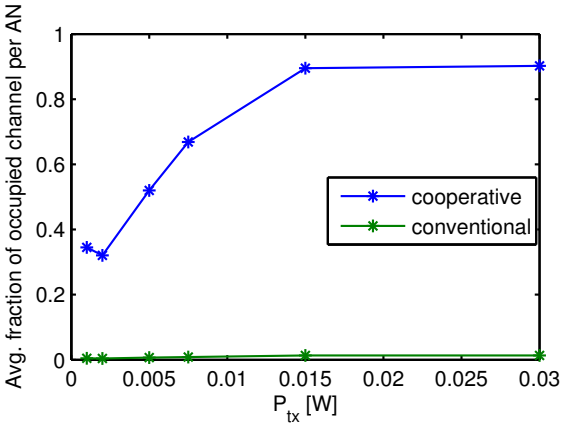

Fig. 11. Average channel occupancy within carrier sense range for varying transmit power level.

We now consider the effect of varying the number of ANs. Fig. 12 shows how the increasing number of ANs causes more traffic in the network. The average occupied channel around the AN can exceed 1 because not all entities are in the same collision domain. That is, multiple transmissions can be ongoing simultaneously if they are spatially well-separated [15].

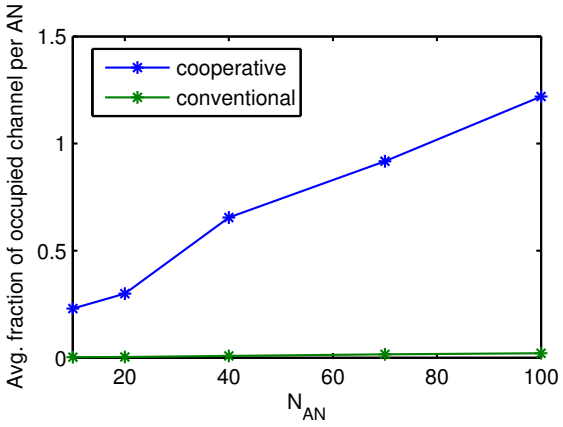

Fig. 12. Average channel occupancy within carrier sense range for varying number of ANs.

Fig. 13 shows the average localization delays for the conventional measurement collection and for the two types of measurements in the cooperative measurement collection. The localization delay is the time it takes from a measurement (received beacon or P2P ranging) is obtained at the MS, until the polling application on the MS has an updated location estimate. The delay for the conventional collection protocol does not change, since its delay only depends on the polling interval of the application μ_{loc}. On the other hand, the delay of the cooperative collection protocol seems to increase slightly with the increase of the number of ANs. If we look at Fig. 12 we see that the channel occupation also increases with the number of ANs, thus the increase in delay may be due to a high level of contention among the network entities. On the other hand, the MS-MS measurements do not seem to be similarly affected by the increasing number of ANs. The reason for the MS-AN measurements being more sensitive to the number of ANs, could also be that many MSs receive the same beacon from an AN and followingly attempt to forward a beacon measurement at the same time. In case the level of contention is already high, the MSs must wait a considerable time to access the channel before the measurement can be delivered to the localization server.

Having presented the behavior of the network when considering realistic communications constraints, we now focus our attention on the positioning algorithms and how the realistic communications constraints affect them.

B. Positioning part

Performance metric is the cumulative distribution function (CDF). The CDF is defined as the probability that the absolute two-dimensional position error is below the value $\varepsilon_{\text{error}}$, i.e.,

$$\text{CDF}\left(\varepsilon_{\text{error}}\right) = \text{Prob}\left(\|\hat{\boldsymbol{x}} - \boldsymbol{x}\|_2 \leq \varepsilon_{\text{error}}\right), \qquad (31)$$

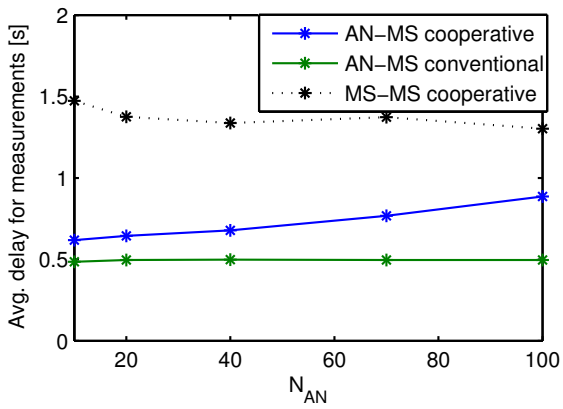

Fig. 13. Average localization delay for varying number of ANs.

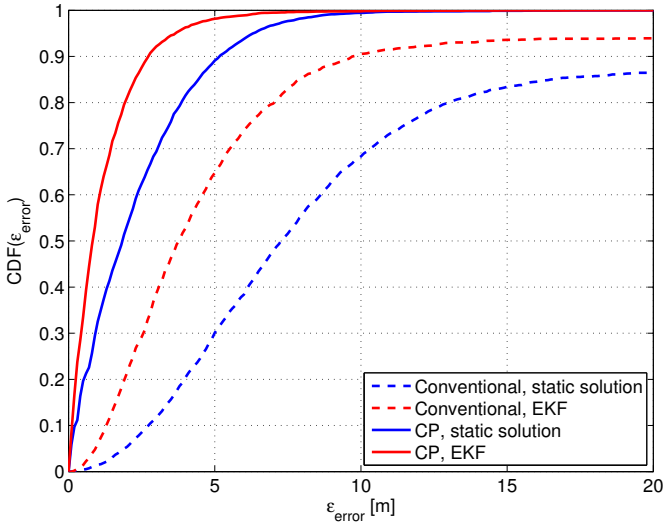

Fig. 14. Conventional vs. cooperative positioning using static solution and EKF.

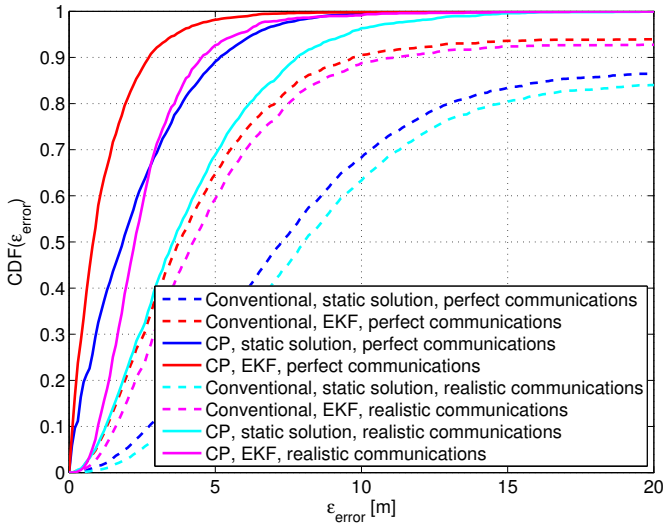

Fig. 15. Conventional vs. cooperative positioning using static solution and EKF with realistic communications constraints.

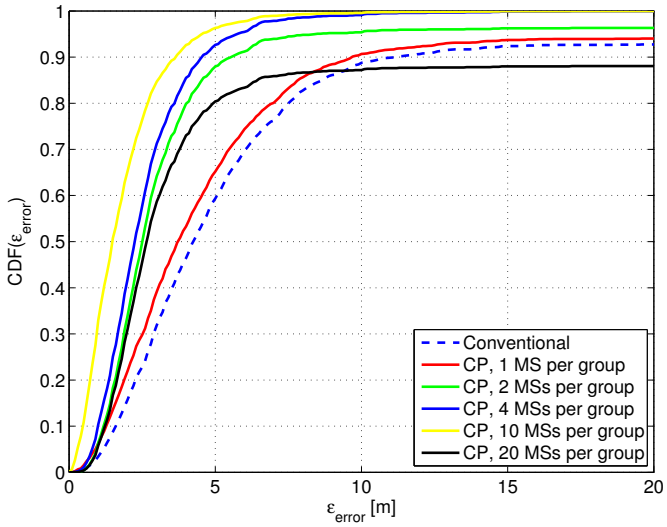

Fig. 16. CP using EKF with realistic communications constraints and different numbers of MS per group.

where it was averaged over all MSs in the scenario and several noise realizations. We further assume that the MS-MS connections are always LOS, whereas the MS-AN connections are NLOS in $50\,\%$ of the cases.

Figure 14 shows the CDF for conventional (non-cooperative) and cooperative positioning for both static solution and tracking with EKF. We observe that for the static solution more than $10\,\%$ of the MSs cannot be localized (e.g., due to limited access to ANs or bad geometric conditions). This can be reduced by application of the EKF resulting in an error being smaller than $10\,\mathrm{m}$ in $90\,\%$ of the cases. If we allow cooperation between the MSs this can further be improved to around $3\,\mathrm{m}$.

Figure 15 includes additionally the results with realistic communications constraints. Here, we observe that the accuracy is decreased by $1\,\mathrm{m}$ in the conventional schemes, whereas it is reduced by around $2\,\mathrm{m}$ and $3\,\mathrm{m}$ for CP using static solution and EKF, respectively. As expected, the loss by communications is higher for the CP scheme compared to the conventional approach. Nevertheless, assuming CP and an EKF the $90\,\%$-error is still below $5\,\mathrm{m}$.

To evaluate the dependency on the MS-MS connectivity, in Figure 16 the number of MSs per group is varied. Note that an increased number of MSs per group automatically results in an increased overall number of MSs N_{MS} since the number of groups is kept constant. We observe that with only one MS per group no noteworthy gains can be achieved by CP compared to the conventional approach. Reason for that is that the connectivity between the groups is only limited. If we increase the number of MSs per group, e.g., to 10, cooperation can be exploited and we achieve an $90\,\%$-error of around $4\,\mathrm{m}$ in this scenario. If we increase it further to 20, it can be seen

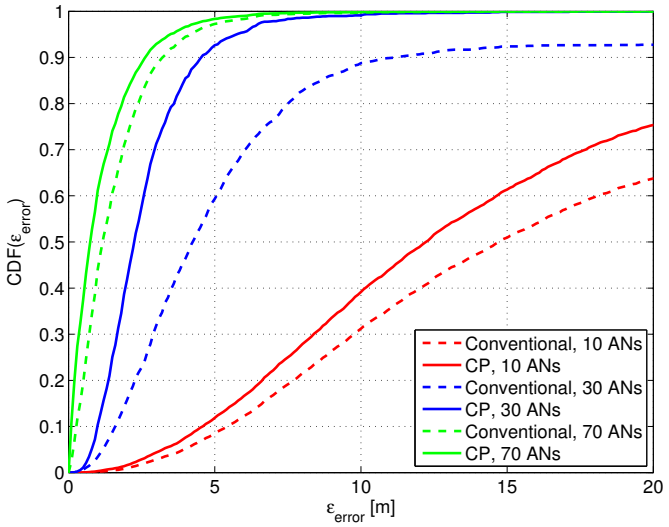

Fig. 17. CP using EKF with realistic communications constraints and different numbers of ANs.

that the performance drops down rapidly, and — in average — around 12 % of the MSs cannot be localized. This could be explained by an increased communications overhead for performing CP with the $N_{\mathrm{MS}} = 120$ MSs and the resulting latency or packet-loss effects.

Figure 17 depicts the dependency on the MS-AN connectivity. For a low number of ANs in the scenario (e.g., 10), several MSs cannot determine their position. In that situation also the cooperation gain is restricted since overall too less ANs are available. On the other hand, if the number of ANs is too high (e.g., 70), the coverage by the ANs limits additional cooperation gains. Therefore, the number of ANs has to be chosen according to the expected MS-MS connectivity in the scenario.

VII. Conclusions

In this paper, we have analyzed cooperative positioning and tracking algorithms under realistic communications constraints. These constraints were modeled here based on a WLAN infrastructure and error models based on empirical measurements. It was shown that the introduction of realistic communications constraints resulted in an added delay, which had a significant effect on the positioning performance, especially for the cooperative algorithms. This is mainly due to the more complex measurement exchange that is necessary to realize the centralized cooperative positioning algorithms. We found that the static solution and the EKF algorithms were similarly affected by the realistic communications constraints. Further, we observed that increasing the number of cooperating MSs had a positive impact on the positioning performance, as expected due to added cooperation possibilities. However, this was only until a tipping point was reached and the performance became worse with additional cooperating MSs. This tipping point is likely a result of the communication overhead becoming large, which in turn leads to increased delays. Nevertheless, in most cases the cooperative approach strongly outperforms the conventional (non-cooperative) approach.

Acknowledgment

This work has been performed in the project WHERE (Grant Agreement number 217033), which is partly funded by the European Union under the European Community's Seventh Framework Programme (FP7/2007-2013).

References

[1] A. H. Sayed, A. Tarighat, and N. Khajehnouri, "Network-Based Wireless Location," *IEEE Signal Processing Magazine*, vol. 22, no. 4, pp. 24–40, July 2005.

[2] P. Misra and P. Enge, *Global Positioning System: Signals, Measurements and Performance*. Ganga-Jamuna Press, 2004.

[3] R. Ercek, P. De Doncker, and F. Grenez, "Study of Pseudo-Range Error Due to Non-Line-of-Sight-Multipath in Urban Canyons," *Proceedings of the ION/GNSS*, pp. 1083–1094, September 2005.

[4] C. L. F. Mayorga, F. della Rosa, S. A. Wardana, G. Simone, M. C. N. Raynal, J. Figueiras, and S. Frattasi, "Cooperative Positioning Techniques for Mobile Localization in 4G Cellular Networks," *Proceedings of the IEEE International Conference on Pervasive Services*, July 2007.

[5] S. Frattasi, "Link Layer Techniques Enabling Cooperation in Fourth Generation Wireless Networks," Ph.D. dissertation, Aalborg University, Aalborg, Denmark, September 2007.

[6] H. Wymeersch, J. Lien, and M. Z. Win, "Cooperative Localization in Wireless Networks," *Proceedings of the IEEE*, February 2009.

[7] F. W. C. Chan and H. C. So, "Accurate Distributed Range-Based Positioning Algorithm for Wireless Sensor Networks," *IEEE Transactions on Signal Processing*, vol. 57, no. 10, pp. 4100–4105, October 2009.

[8] S. M. Kay, *Fundamentals of Statistical Signal Processing: Estimation Theory*. Prentice Hall, 1993.

[9] F. Gustafsson and F. Gunnarsson, "Mobile Positioning Using Wireless Networks," *IEEE Signal Processing Magazine*, vol. 22, no. 4, pp. 41–53, July 2005.

[10] T. Perälä and R. Piché, "Robust Extended Kalman Filtering in Hybrid Positioning Applications," *Proceedings of the Workshop on Positioning, Navigation and Communication (WPNC)*, March 2007.

[11] Q. Chen, F. Schmidt-Eisenlohr, D. Jiang, M. Torrent-Moreno, L. Delgrossi, and H. Hartenstein, "Overhaul of IEEE 802.11 modeling and simulation in ns-2," *Proceedings of the 10th ACM Symposium on Modeling, analysis, and simulation of wireless and mobile systems*, 2007.

[12] "Wireless lan medium access control (mac) and physical layer (phy) specifications," *IEEE Std 802.11-2007 (Revision of IEEE Std 802.11-1999)*, pp. C1–1184, 12 2007.

[13] M. Pezzin and A. Alvarez Vazquez, "Real Life Ranging Measurements with Low Power, Low Data Rate Transceivers," *Proceedings of the Workshop on Positioning, Navigation and Communication (WPNC)*, March 2010.

[14] M. Raspopoulos, S. Stavrou, B. Uguen, R. Burghelea, M. García, T. Pedersen, G. Steinböck, B. H. Fleury, B. Denis, J. Youssef, Y. Lostanlen, and Álvaro Álvarez, "WHERE D4.3 v1.1 - Modelling of the Channel and its Variability," ICT-217033 WHERE, Tech. Rep., 2009.

[15] T. Kim, H. Lim, and J. Hou, "Improving spatial reuse through tuning transmit power, carrier sense threshold, and data rate in multihop wireless networks," in *Proceedings of the 12th annual international conference on Mobile computing and networking*. ACM, 2006, p. 377.